Supporting Information (SI) Section

Photochemistry of Products of the Aqueous Reaction of Methylglyoxal with Ammonium Sulfate

Paige K. Aiona, [1] Hyun Ji (Julie) Lee,[1] Renee Leslie,[1] Peng Lin,[2] Alexander Laskin,[3] Julia Laskin,[3] and Sergey A. Nizkorodov[1,*]

1. *Department of Chemistry, University of California, Irvine, California 92697, USA.*
2. *Environmental Molecular Sciences Laboratory, Pacific Northwest National Laboratory, Richland, Washington 99352, USA.*
3. *Department of Chemistry, Purdue University, West Lafayette, Indiana 47907 USA.*

* Corresponding author phone and e-mail: 949-824-1262, nizkorod@uci.edu

Contents

Calculation of the Effective Quantum Yield of Photolysis

The effective photolysis quantum yield was calculated as the ratio of the rate of photolysis ($Rate_{photolysis}$) to the effective rate of photon absorption ($Rate_{absorption}$):

$$QY = \frac{Rate_{photolysis}}{Rate_{absorption}} \qquad \text{(S1, same as Eq. 2)}$$

$Rate_{absorption}$ by the solution was calculated from the base-10 wavelength-dependent absorbance $A_{vertical}(\lambda)$ through the solution of height $h_{solution}$, and from the spectral flux density of the photolyzing radiation, $D_0(\lambda)$, as described in Lee et al. (2014).[1]

$Rate_{photolysis}$ can be determined from the rate of change of absorbance of the solution at a chosen probe wavelength. However, this is complicated by the fact that both the initially present BrC compounds and their photolysis products also absorb at the probe wavelength. It is instructive to first consider what happens in the case of a single absorbing compound *R* producing a single product *P* with a photolysis rate constant *k*. We assume that both *R* and *P* absorb at the probe wavelength with molar extinction coefficients ε_R and ε_P, respectively. In this case, the absorbance changes with time as follows:

$$A(t) = b[R]_0\left[\varepsilon_P + \left(\varepsilon_R - \varepsilon_P\right)e^{-kt}\right] \qquad \text{(S2)}$$

Fitting the absorbance to function

$$A(t) = c_1 + c_2 e^{-kt} \qquad \text{(S3)}$$

with c_1, c_2, and *k* as fitting parameters should give us the effective rate constant, *k*, and therefore the photolysis rate:

$$Rate_{photolysis} = k[R]\frac{N_A}{1000} \qquad \text{(S4)}$$

The Avogadro number and the factor of 1000 appearing in this equation are for converting the molar concentrations into molecular units compatible with equation (S1).

To avoid complications associated with the rate of absorption changing with photolysis time, both absorption and photolysis rates were evaluated at t=0 when the initial molar concentration of the reactant and the absorbance of the solution are related via:

$$A_0 = b\varepsilon_R[R]_0 \qquad \text{(S5)}$$

The BrC extract contains a number of compounds, and there is no reason to expect that the absorbance of the solution should follow first-order kinetics expected from equation (S2). However, the observed decay in absorbance appeared to fit an exponential decay reasonably well, as shown in Figure 1 of the manuscript. Therefore, in this work, we approximated the BrC mixture as a solution of a single organic compound with an average formula and average optical properties of BrC. Taking the average molecular weight (*MW*) for the BrC molecules from the HR-MS data we converted the mass concentration (C_{mass}) of the dissolved BrC into the effective molar concentration:

$$[R]_0 = \frac{C_{mass}}{MW} \tag{S6}$$

The concentration in the above equations was then used to calculate the effective quantum yield of photolysis at t=0.

Figure S1. Spectral flux density of radiation, $D_0(\lambda)$, from the irradiation source compared to that from the sun at different solar zenith angles (SZA).

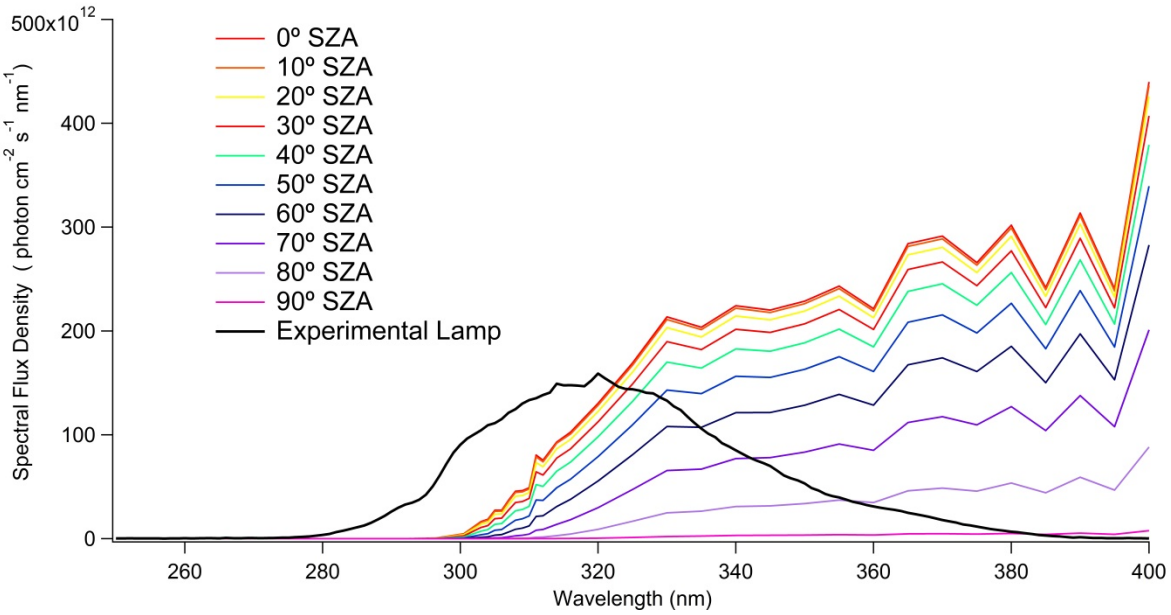

Table S1. The list of assigned HR-ESI-MS peaks with significant abundance

Molecular weights, MW, in Dalton (Da) and the formulas are listed for all assigned peaks. In the "Trend" column, decrease in intensity (↓), increase in intensity (↑), and no change (–) in response to photolysis are listed. Also, peaks found only before or after photolysis are listed as B or A, respectively. The IC + MG oligomers highlighted are bolded and labelled with letter "O" in the last column.

MW (Da)	C	H	N	O	Trend	Olig
124.0637	**C_6**	**H_8**	**N_2**	**O_1**	↓	**O**
126.0317	C_6	H_6		O_3	↓	
127.0633	C_6	H_9	N_1	O_2	↓	
128.0473	C_6	H_8		O_3	↓	
130.0630	C_6	H_{10}		O_3	↓	
140.0586	C_6	H_8	N_2	O_2	A	
143.0582	C_6	H_9	N_1	O_3	↓	
150.0793	C_8	H_{10}	N_2	O_1	↑	
151.0633	C_8	H_9	N_1	O_2	↓	
152.0950	C_8	H_{12}	N_2	O_1	↑	
168.0899	C_8	H_{12}	N_2	O_2	↑	
170.0579	C_8	H_{10}		O_4	↓	
177.0902	C_9	H_{11}	N_3	O_1	↓	O
178.0742	C_9	H_{10}	N_2	O_2	↑	O
186.0528	C_8	H_{10}		O_5	↓	
194.0691	C_9	H_{10}	N_2	O_3	↓	O
196.0848	**C_9**	**H_{12}**	**N_2**	**O_3**	↓	**O**
197.0688	C_9	H_{11}	N_1	O_4	↓	
198.0528	C_9	H_{10}		O_5	↓	
198.1004	C_9	H_{14}	N_2	O_3	↑	
200.0685	C_9	H_{12}		O_5	↓	
202.0954	C_8	H_{14}	N_2	O_4	A	
212.1161	C_{10}	H_{16}	N_2	O_3	↑	
214.0954	C_9	H_{14}	N_2	O_4	↑	
215.0794	C_9	H_{13}	N_1	O_5	–	
222.1004	C_{11}	H_{14}	N_2	O_3	↑	
231.1008	C_{12}	H_{13}	N_3	O_2	↓	O
232.0848	C_{12}	H_{12}	N_2	O_3	↑	O
233.0899	C_9	H_{15}	N_1	O_6	–	
240.1110	C_{11}	H_{16}	N_2	O_4	↑	
248.1273	C_{12}	H_{16}	N_4	O_2	↓	
249.1113	C_{12}	H_{15}	N_3	O_3	↓	O
250.0954	C_{12}	H_{14}	N_2	O_4	↓	O
250.1430	C_{12}	H_{18}	N_4	O_2	↑	
252.1110	C_{12}	H_{16}	N_2	O_4	↓	
266.0903	C_{12}	H_{14}	N_2	O_5	↓	O
268.1059	**C_{12}**	**H_{16}**	**N_2**	**O_5**	↓	**O**
269.0899	C_{12}	H_{15}	N_1	O_6	↓	
271.1056	C_{12}	H_{17}	N_1	O_6	↓	

278.0862	C_{8}	H_{14}	N_{4}	O_{7}	↑		
286.1165	C_{12}	H_{18}	N_{2}	O_{6}	↓		
287.1005	C_{12}	H_{17}	N_{1}	O_{7}	↓		
288.0845	C_{12}	H_{16}		O_{8}	↓		
289.1162	C_{12}	H_{19}	N_{1}	O_{7}	↑		
304.1271	C_{12}	H_{20}	N_{2}	O_{7}		B	O
305.1111	C_{12}	H_{19}	N_{1}	O_{8}	↑		
305.1376	C_{15}	H_{19}	N_{3}	O_{4}	↓		O
307.1267	C_{12}	H_{21}	N_{1}	O_{8}	↓		
313.1162	C_{14}	H_{19}	N_{1}	O_{7}	↓		
322.1165	C_{15}	H_{18}	N_{2}	O_{6}	↓		O
323.1216	C_{12}	H_{21}	N_{1}	O_{9}	↓		
340.1271	C_{15}	H_{20}	N_{2}	O_{7}	↓		
341.1111	**C_{15}**	**H_{19}**	**N_{1}**	**O_{8}**	**↓**		**O**
358.1376	C_{15}	H_{22}	N_{2}	O_{8}	↓		
359.1216	C_{15}	H_{21}	N_{1}	O_{9}	↓		
361.1373	C_{15}	H_{23}	N_{1}	O_{9}	↓		
376.1271	C_{18}	H_{20}	N_{2}	O_{7}	↓		O
377.1322	C_{15}	H_{23}	N_{1}	O_{10}	↓		
393.1536	C_{18}	H_{23}	N_{3}	O_{7}	↓		O
394.1376	C_{18}	H_{22}	N_{2}	O_{8}	↓		O
395.1428	C_{15}	H_{25}	N_{1}	O_{11}	↓		
412.1482	**C_{18}**	**H_{24}**	**N_{2}**	**O_{9}**	**↓**		**O**
466.1587	C_{21}	H_{26}	N_{2}	O_{10}	↓		O
484.1693	**C_{21}**	**H_{28}**	**N_{2}**	**O_{11}**	**↓**		**O**

Suggested Structures of the Observed Oligomeric Compounds

Scheme S1. Possible Imidazole and Imidazole-Pyrrole Oligomers

Examples of imidazole and imidazole-pyrrole oligomers. The structures are tentative and based on observed patterns in the ESI-HRMS mass spectra.

(a). C12 oligomers (tetramers)

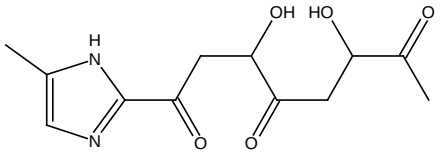

$C_{12}H_{16}N_2O_5$ (MW 268.11)

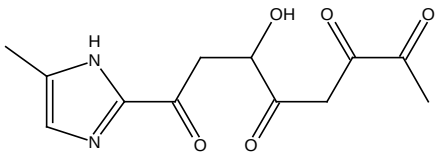

$C_{12}H_{16}N_2O_5$ (MW 266.09)

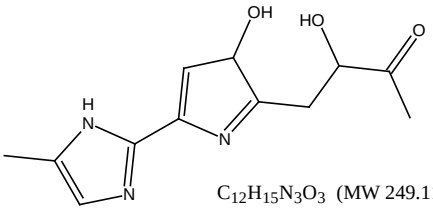

$C_{12}H_{15}N_3O_3$ (MW 249.11)

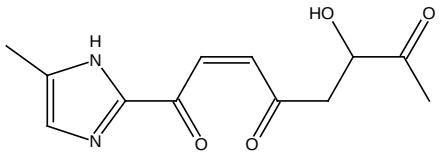

$C_{12}H_{14}N_2O_4$ (MW 250.10)

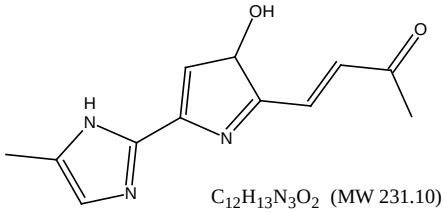

$C_{12}H_{13}N_3O_2$ (MW 231.10)

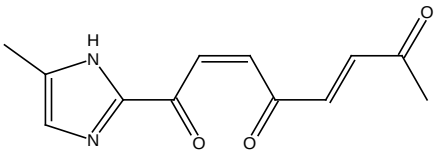

$C_{12}H_{12}N_2O_3$ (MW 232.08)

(b). C15 oligomers (pentamers)

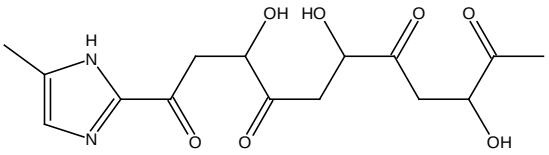

$C_{15}H_{20}N_2O_7$ (MW 341.13)

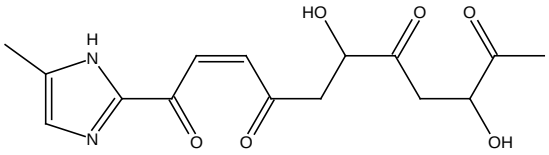

$C_{15}H_{18}N_2O_6$ (MW 322.12)

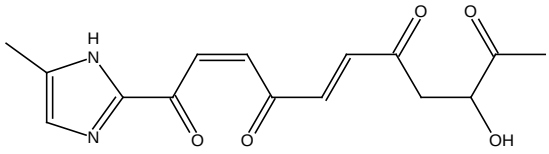

$C_{15}H_{16}N_2O_5$ (MW 304.11)

(c). C18 oligomers (hexamers)

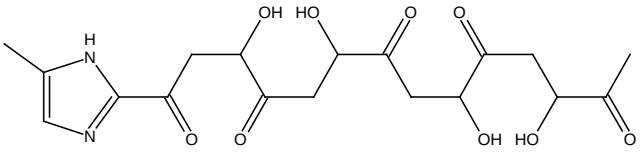

$C_{18}H_{24}N_2O_9$ (MW 412.15)

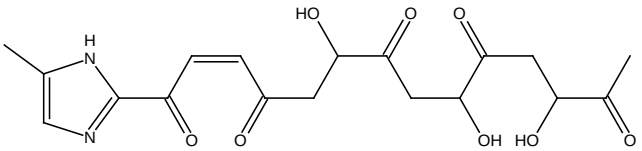

$C_{18}H_{22}N_2O_8$ (MW 394.14)

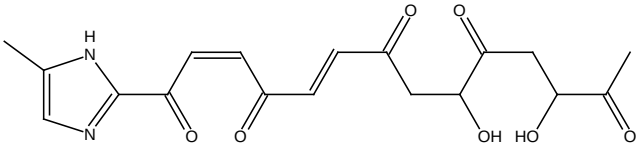

$C_{18}H_{20}N_2O_7$ (MW 376.13)

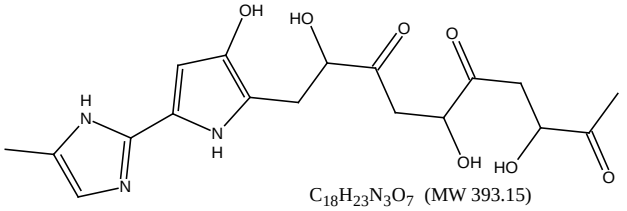

$C_{18}H_{23}N_3O_7$ (MW 393.15)

(d). C21 oligomers (heptamers)

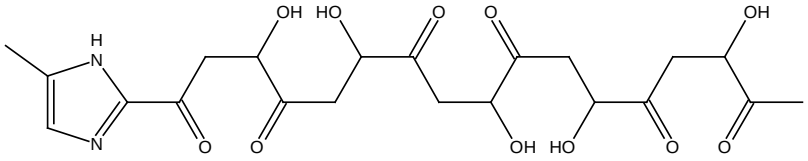

$C_{21}H_{28}N_2O_{11}$ (MW 484.17)

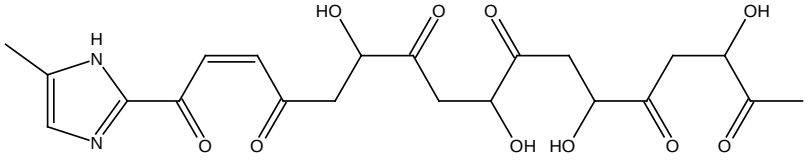

$C_{21}H_{26}N_2O_{10}$ (MW 466.16)

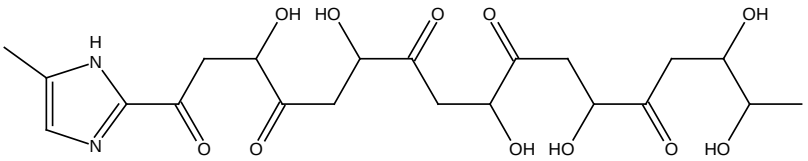

$C_{21}H_{30}N_2O_{11}$ (MW 486.18)

Double Bond Equivalents of BrC Compounds

For compounds, $C_cH_hO_oN_n$, containing *c* carbon, *h* hydrogen, *o* oxygen, and *n* nitrogen atoms, the double bond equivalent (DBE), which is equal to the total number of double bonds and rings, can be calculated as follows:

$$DBE = 1 + \frac{n - h}{2} + c \quad \text{(S7)}$$

Nitrogen is assumed to have a valence of 3 in this formula, which is consistent with its anticipated chemistry. The distribution of DBE values in the MG/AS BrC is shown in Figure S2.

Figure S2. DBE of MG/AS BrC products.

DBE is plotted as a function of the carbon number before and after photolysis. The size of the points represents relative intensity. The dashed line corresponds to the expected DBE for linear polyenes (C_xH_{x+2}).

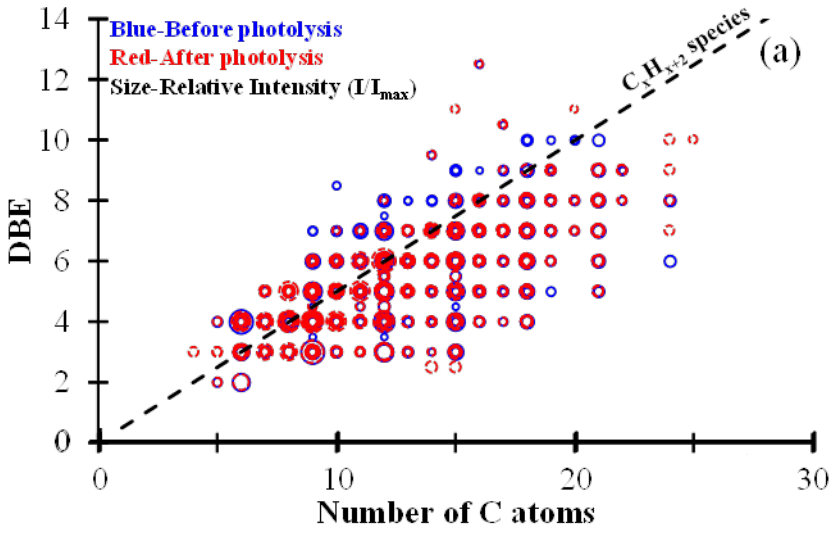

Elemental Composition of BrC

Average elemental ratios are commonly used to express bulk composition for comparing the complexity of the SOA. Using the assigned molecular formulas, the average elemental composition (C, H, N, and O), ratios (H/C, O/C, N/C, and N/O), and DBE are estimated based on the following equations:

$$\langle Y \rangle = \frac{\sum_i x_i Y_i}{\sum_i x_i} \qquad \text{where Y= c, h, o, n, DBE} \tag{S8}$$

$$\frac{\langle Y \rangle}{\langle Z \rangle} = \frac{\sum_i x_i Y_i}{\sum_i x_i Z_i} \qquad \text{where Y/Z = H/C, O/C, N/C, and N/O} \tag{S9}$$

Peak abundance, x_i, is used as the weighing factor. Table S2 lists all the calculated average elemental ratios and DBE for MG/AS BrC samples before and after photolysis. Table S3 focuses on the fraction of N-containing compounds and the N/C ratios for the subgroups of the compounds containing n = 0, 1, 2, 3, and 4 N-atoms.

Table S2. Elemental composition of BrC

Average elemental ratios and double-bond equivalents (DBE) before and after photolysis.

	<H/C>	<O/C>	<N/C>	<N/O>	<DBE>
Before	**1.47**	**0.51**	**0.14**	**0.28**	**3.9**
(SD)	(0.03)	(0.03)	(0.03)	(0.07)	(0.5)
After	**1.53**	**0.50**	**0.15**	**0.32**	**3.7**
(SD)	(0.04)	(0.10)	(0.04)	(0.1)	(0.7)
After - Before	**0.06**	**-0.01**	**0.003**	**0.04**	**-0.2**

Table S3. Nitrogen-containing compounds in BrC

Percent of N-containing compounds and the average N/C ratio for each subset of N-containing compounds (with n=0, 1, 2, 3, and 4) before and after photolysis.

# N	%		<N/C>	
	Before	**After**	**Before**	**After**
0	22.6	20.7		
1	43.5	42.9	0.08	0.08
2	25.5	30.7	0.21	0.21
3	5.6	3.7	0.20	0.21
4	2.7	2.0	0.49	0.35
sum	**100.0**	**100.0**		

HPLC-PDA-HRMS data

Figure S3. SIC for *m/z* 125.0709 ion (IC)

The selected Ion Chromatogram (SIC) for the *m/z* 125.0709 ion (mass range 125.00-125.10) corresponding to protonated IC is shown in the bottom of the first panel. The 12.2 min peak in SIC (bottom) correlates with the 11.8 min peak of the major chromophore in the PDA chromatogram (top). Other peaks in SIC may be due to less stable isomers of IC (see Scheme 2 in the text) or fragmentation of larger compounds into protonated IC. The second panel shows the full absorption spectrum of the peak at 11.8 minutes in the PDA with a broad peak centered around 290 nm.

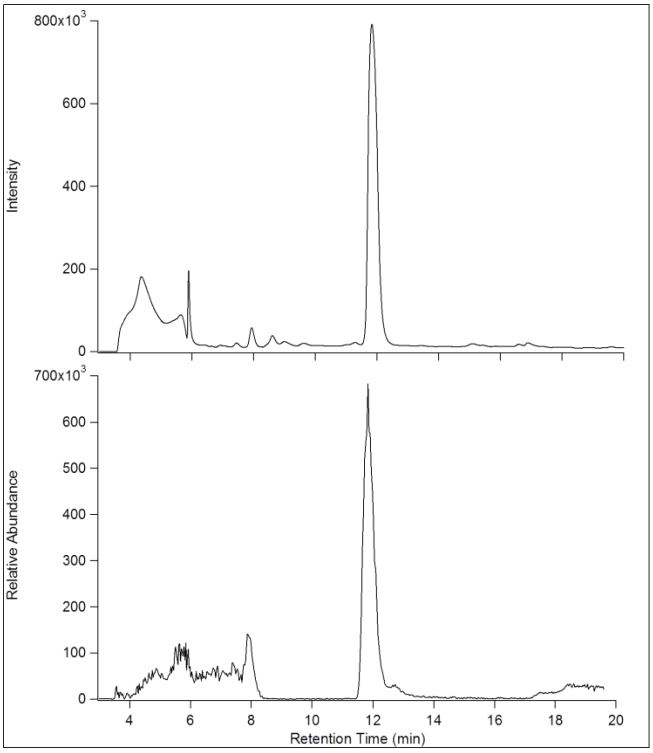

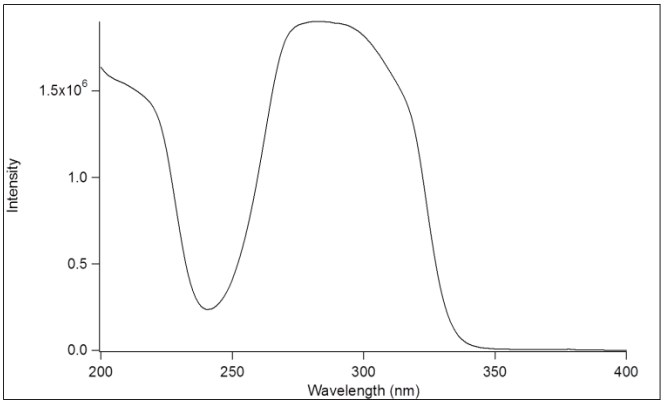

Figure S4. Comparison between PDA chromatograms for MG/AS BrC prepared by evaporation and by aqueous reaction

The top PDA chromatogram corresponds to a BrC sample obtained by Lin et al.[2] by a reaction of MG with AS in water for four days followed by desalting to remove excess AS. The bottom chromatogram was obtained for an evaporation MG/AS BrC sample, with no desalting used. While the major peak of IC is the same in both cases, there are very significant differences between the distributions of eluting BrC chromophores in the two samples.

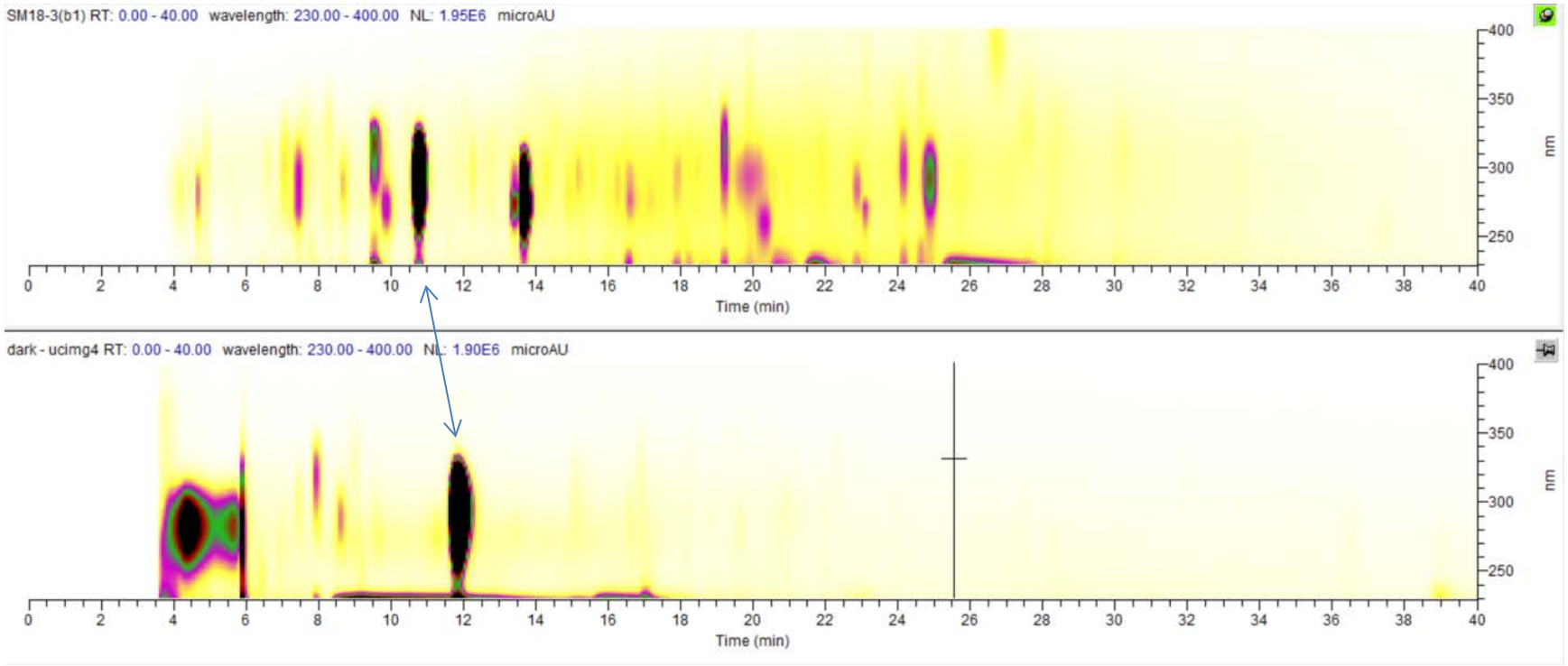

Scheme S2. Formation of non-chromophoric compounds observed in HPLC-PDA-HRMS

Possible mechanism for the formation of the observed products that are not derived from imidazole. MG and hMG stand for methylglyoxal and hydrated methylglyoxal, respectively.

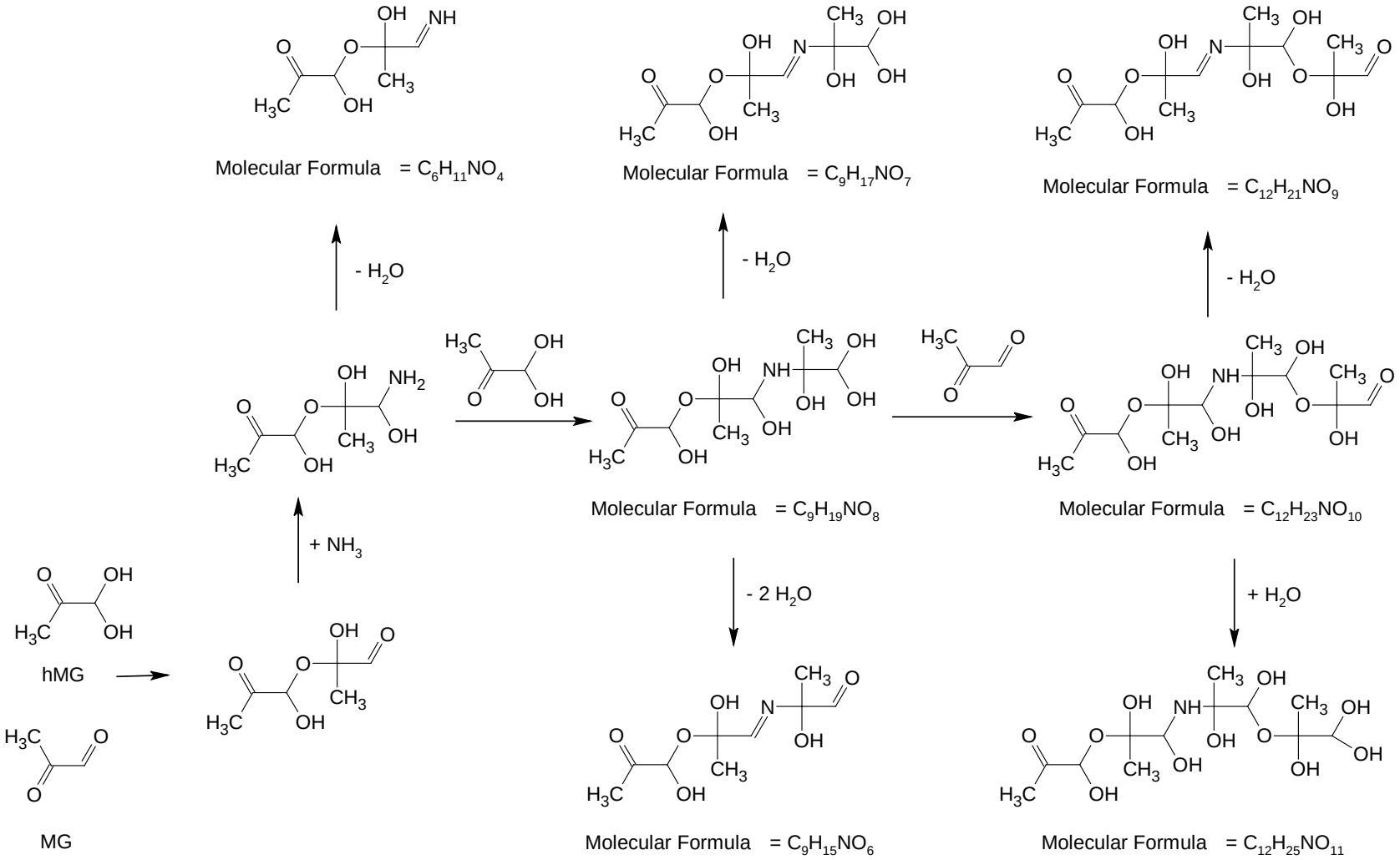

References:

1. Lee, H. J.; Aiona, P. K.; Laskin, A.; Laskin, J.; Nizkorodov, S. A., Effect of solar radiation on the optical properties and molecular composition of laboratory proxies of atmospheric brown carbon. *Environ. Sci. Technol.* **2014,** *48*, (17), 10217-10226.
2. Lin, P.; Laskin, J.; Nizkorodov, S. A.; Laskin, A., Revealing brown carbon chromophores produced in reactions of methylglyoxal with ammonium sulfate. *Environ. Sci. Technol.* **2015,** *49*, (24), 14257-14266.